Penerbit Akademia Baru

Journal of Advanced Research in Fluid Mechanics and Thermal Sciences

Journal homepage: www.akademiabaru.com/arfmts.html
ISSN: 2289-7879

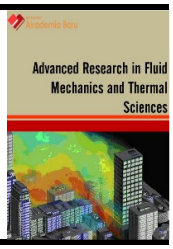

OpenFOAM Implementation for The Study of Streamwise Vortex-Induced Vibration-Based Energy Harvester for Sensor Networks

Open Access

Ahmad Adzlan Fadzli Khairi[1,2,*], Mohamed Sukri Mat Ali[1]

[1] Wind Engineering for Environment Laboratory, Malaysia-Japan International Institute of Technology, Universiti Teknologi Malaysia, 54100, Kuala Lumpur, Malaysia
[2] Department of Mechanical and Manufacturing Engineering, Faculty of Engineering, Universiti Malaysia Sarawak, 94300 Kota Samarahan, Sarawak, Malaysia

ARTICLE INFO

Article history:
Received 25 May 2018
Received in revised form 22 July 2018
Accepted 14 August 2018
Available online 16 August 2018

Keywords:
OpenFOAM, vortex shedding, vortex induced-vibration, streamwise vortices

ABSTRACT

The study of streamwise vortex induced vibration has reached a level of maturity that allows it to be harnessed to generate power. However, studies have primarily concentrated on the variables that measured through point-based instruments. This severely limits our understanding of the fluid forcing mechanism that results in the vibration of the elastically supported bluff body. We proposed the usage of computational fluid dynamics: the open source C++ libraries of OpenFOAM. To implement this successfully to the streamwise vortex-induced vibration problem, which involves near-wall fluid-structure interaction, we explored the method of dynamic mesh handling in OpenFOAM for six degrees of freedom motion of a rigid body fully submerged in fluid. Finally, we argued for the usage of arbitrarily coupled mesh interface to overcome the problem of severely distorted mesh in tight gaps between two walls. We run a short simulation to test this setup and found that the case runs uninterrupted, unlike its former counterpart that relies solely on cell displacement diffusion, suggesting the potential success of a further converged solution of the setup when running on a more powerful machine.

1. Introduction

1.1 Off-Grid Operation of Sensor Networks

The growing demand for real-time monitoring and management of agriculture [29], civil structures [44], machinery [9], and hydrological systems [5] led towards widespread adoption of sensors networks in these disciplines. Under the desired operating conditions, most of the application of the sensors are at sites where power from the national grid is either difficult to source, or non-existent. Sometimes, the issue is not so much on the fact that power lines from the national grid are out of reach, as it is related to the involvedness of the means to distribute the power, e.g.,

* *Corresponding author.*
E-mail address: kaafadzli@unimas.my (Ahmad Adzlan Fadzli Bin Khairi)

installing/extending power lines, or connecting the power line to the sensor, e.g., for cases where sensors are embedded inside bridges.

Off-grid alternatives for power generation for sensor networks typically rely on one form or another of renewable energy technology. River monitoring in Malaysia, for example, uses solar photovoltaic (PV) panels to power their water depth and discharge sensors. The usage of a renewable energy source relieves the designer of a sensor network not only from the cost, but also the bureaucracy involved in sourcing power from the national grid - especially when the sensor network is to collect data in remote areas.

For a wide range of operating locations, solar PV panels provide a reliable and economic renewable energy solution to the power source problem for sensor networks. However, PV panels need batteries as part of the power system to be able to provide continuous power to the sensors. This is going to be a problem in the future because the number of sensor networks can only be expected to grow. The growth is foreseeable because: (1) more parties are acknowledging sensor networks as being an integral part of the internet of things (IoT) [42], and (2) there is a renewed effort to automate and remotely control aspects of our industrial practices - including agriculture e.g., intelligent palm pollination and shrimp farm management [29].

If solar PV panels become the only go-to technology for renewable energy generation, we must be prepared to face several challenges, one being the disposal of the used batteries [9], and second is theft of the solar PV panels themselves [3,4]. We can avoid these problems by opting for an alternative renewable energy technology, such as hydropower generation. Considering the power requirement for sensors are generally low (<1 W), the method to be employed only needs to: (1) generate that much power, (2) continuously, (3) using inexpensive materials that do not incentivize its theft. Power generation via streamwise vortex-induced vibration (SVIV) is a method that fulfils all the criteria listed above.

1.2 Hydropower Generation by Exploiting SVIV

Streamwise vortex-induced vibration (SVIV) is the name given to the vibration of a cylindrical bluff body that is caused by the alternate shedding of streamwise vortex pairs from the top and bottom surfaces of the cylinder [32,45]. While the type of vortex shedding from an immersed cylindrical bluff body is typically the Karman vortex, whose vortex axis is parallel to the cylindrical axis (lateral vortex), the streamwise vortex pairs have their axis perpendicular to the axis of the cylinder. The appearance of the streamwise vortex from the cylinder is toggled by placing another cylindrical bluff body downstream perpendicularly, at a certain range of gaps [6,15,36] between the upstream and downstream cylinders.

There are two forms of streamwise vortices that have been observed: the trailing and necklace vortices. Both exhibit the ability to lock-in to the natural frequency of the system [26], thus generating energetic vibration that is key to energy harvesting. A schematic of these two vortices is given in Fig. **1**.

Sensor networks are required to: (1) operate continuously with (2) minimal maintenance [14]. Therefore, the power supply to the sensor network must be robust, with a minimal component count and simple geometric design. To further simplify the geometric design of the SVIV oscillator, Kawabata *et al.,* [17] and Koide *et al.,* [19] replaced the downstream cylinder with a strip-plate, i.e. a thin rectangular cylinder, and studied its amplitude and frequency responses. These studies demonstrated the ability to initiate the formation of the streamwise vortices are not strictly dependent on the geometric design of the cylinders - both upstream and downstream. Using the

strip-plate also expands the range of velocity that sustains SVIV, in addition to higher amplitude response, compared to a circular downstream cylinder [18].

A laboratory scale energy harvester that utilizes SVIV was developed and tested by Koide *et al.,* [21] and Koide *et al.,* [22]. The energy harvester exhibits constant power magnitude over a sizeable range of velocities ($1 < U\ (\mathrm{m/s}) < 4$) for a circular cross-section oscillator of diameter 10 mm, length 980 mm, mass ratio $m^* = 17.43$, and Scruton number 7.74. The mass ratio gives the ratio of the mass of the vibrating system to the mass of fluid displaced by the oscillating cylinder, i.e. $m^* = m_{\mathrm{system}}/m_{\mathrm{displaced}} = m_{system}/(\pi D^2 L/4)$, with *D* and *L* being the diameter and length of a circular cylinder. The Scruton number Sc is a way to quantify the mass and damping of a vibrating system and it is given by $Sc = 2m^*\delta$, where δ is the logarithmic decrement of the system.

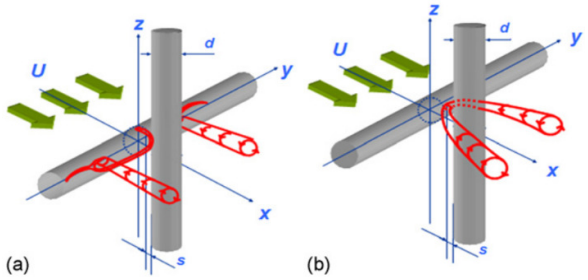

Fig. 1 Schematic of the two forms of the streamwise vortex: (a) trailing vortex and (b) necklace vortex [27]

The sizeable operating velocity range partially fulfils the constant operations requirement, and constant power output within this velocity range implies an inherent power regulating mechanism in the system. However, the onset velocity for SVIV in water of about 1 m/s, and the magnitude of power generated currently in the order of mW, usage of the SVIV-based energy harvester remains constrained to singular sensors only. Powering whole sensor networks including the transmission and reception of collected data is still elusive due to insufficient power. To overcome these shortcomings, parametric studies on SVIV control are imperative, and the avenues already explored are reviewed in the next section.

The objectives of this work are threefold: (1) to review the literature and examine the parameters that affect SVIV, (2) to establish the worthwhileness of computational fluid dynamics (CFD) in the study of SVIV, particularly one that uses the open source software OpenFOAM, and (3) to check whether our case set up for an SVIV simulation using arbitrarily coupled mesh interface (ACMI) can run without encountering errors.

2. Literature review

2.1 Aspects of SVIV Control

The cruciform arrangement of cylindrical bluff bodies was initially investigated to control the behaviour of Karman vortices from pipe-like structures, the shedding of which causes disruptive vibrations. This method of vibration control does not require any modifications to the pipe-like structures, and the flow upstream the cylinder is virtually left unperturbed - making it relatively simple to retrofit to already existing systems.

However, at certain gaps between the upstream and downstream cylinder in a cruciform arrangement, another type of vortex shedding occurs, whose Strouhal number is 3 to 7 times smaller compared to the Karman vortex. This is true in the two circular cylinders in the cruciform arrangement by Shirakashi *et al.,* [32]. When the flow is visualized using smoke streaks in a wind

tunnel, the axis of rotation of the vortices being shed was found to be parallel to the free stream (perpendicular to the upstream cylinder axis), hence the name streamwise vortex. The following are several parameters that were found to affect aspects of SVIV.

The normalized gap s^* ($= s/D$, s being the gap between the upstream and downstream cylinder) plays a critical role in the control of streamwise vortices. The two documented forms of streamwise vortex, trailing and necklace, is contingent on s^*. The trailing vortex for example, appears when $0 < s^* < 0.25$, and the necklace vortex when $0.25 < s^* < 0.5$, as observed in the wind tunnel experimented by Bae *et al.,* [7], studying the cruciform arrangement of two circular cylinders. The nondimensional vibration amplitude z^* ($= z/D$, where z is the transverse displacement of the upstream cylinder) is also influenced by s^*. There is a region of high z^* when $s^* < 0.3$ both at VIV and galloping regions [21].

On the other hand, Reynolds number, Re was observed to affect the nondimensional frequency of vortex shedding, i.e. Strouhal number (St=fD\/U, where f and U are the characteristic frequency and velocities respectively). St increases with increasing Re when $\mathrm{Re} < 10000$. However, St ceases to change when $\mathrm{Re} > 10000$ [6]. Similar experiments were repeated in wind tunnels of different dimensions, and in a water tunnel. The results showed good reproducibility in both mediums [20].

Mass-damping parameter - or its nondimensional equivalent - Scruton number, Sc, is commonly related to the maximum amplitude and frequency responses of any VIV system. For SVIV, there is a notable lack of data for systematic variation of the mass ratio m^*, and damping δ, most probably due to the exceptionally high initial investment in manpower and capital in developing a cyber-fluidic system that can vary m^* and δ independently [23,35,34]. VIV studies that did pursue the effects of mass-damping without cyber-fluidic systems rely on nondimensionalizing these quantities to allow comparison between experimental runs [22,27]. Nevertheless, a subtle trend has been pointed out as reported by Nguyen *et al.,* [27] with respect to damping: the maximum amplitude (frequency) decreases (increases) with increasing damping.

2.1 Implementation of Computational Fluid Dynamics (CFD) In SVIV Studies

Although the research highlighted above study important aspects of SVIV, they invariably leave out the examination of quantities whose measurement require 2 dimensional (2D) snapshots of the instantaneous velocity field. Example of such quantities is vorticity, circulation, meandering of the separation point (for circular cylinders), reattachment length, and momentum thickness. The best tool available to the researcher for the above purpose is 2D particle image velocimetry (PIV) [16,40]. A well-calibrated PIV system enables the collection of time-resolved 2D velocity fields to an uncertainty level of less than 5% [43].

Despite this, there is a paucity of the adoption of PIV in SVIV studies, perhaps due to the prohibitive cost of procuring such a system. An alternative is to solve for the flow field variables using computational fluid dynamics (CFD).

CFD is the discipline of solving the governing equations of fluid dynamics using numerical methods and approximations. In principle, end users only need: (1) a computer and (2) a solver program to start their practice of CFD. With household access to computers in Malaysia now nearing 70% of the population [11] and near-ubiquitous availability of computers in higher education institutions, requirement (1) for CFD practice can be fulfilled with a modest effort from the researcher. Fulfillment of requirement (2) is even more straightforward: end users can download and install the OpenFOAM [28], C++ libraries and begin developing their simulation case right away.

OpenFOAM is highly customizable as it is open-source, and the general public license (GPL) under which it is distributed means that anybody can use it for free. All solver applications in OpenFOAM

can be run in parallel, which is indispensable when tackling computationally demanding projects. Parallelization allows the pooling of existing computing resources instead of procuring new ones, aiding initial adoption cost reduction.

Simulation of SVIV using CFD allows detailed analysis of the instantaneous three-dimensional (3D) flow field around the cylinders. To ensure the validity of the simulation, the case must be set up to mimic the real-world conditions as faithfully as possible, while keeping the computational cost at a minimum. Here we note that the phenomenon of SVIV is a 3D, transient, turbulent, fluid-structure interaction (FSI), where the flow influences the motion of the structure and vice-versa. Since there is a marked lack of CFD work in the literature that deals with SVIV, especially ones that employ OpenFOAM, we first need to determine how to implement the features of SVIV into our simulation - most importantly FSI handling and turbulence modelling. Relevant literature on these subjects is reviewed in the following subsections.

2.2 General FSI Handling in OpenFOAM

Numerical solution of partial differential equations involves the discretization of the independent variables, both spatial and temporal. Among these two, discretizing the spatial extent of the simulation is usually more demanding, and calls for a substantial degree of physical insight. Discretization of the spatial extent of the simulation is commonly referred to as meshing, and this discipline continues to be in active development to this day [30,31].

We want to point out that there only exists a limited amount of documentation for dynamic mesh handling in OpenFOAM [24]. This lack of documentation, compared to proprietary software, is the earmark open source technology. The common wisdom is that because we can look at the source code, multi-volume documentation of the software is not necessary. Short of going through the source code, users generally figure their way to set up their simulation case by (1) inspecting existing tutorial cases included in their OpenFOAM installation, (2) reading the error messages (3) posting their queries on forums, e.g. CFD Online, and (4) referring to case setups shared by other OpenFOAM users. We follow the same steps in this review as well.

A simulation that involves the movement of a rigid body inside a flow requires the surrounding mesh to be able to absorb and follow the motion while retaining the quality of the mesh within an acceptable level, quantified by mesh metrics such as skewness and orthogonality [2]. In OpenFOAM, handling of mesh motion, i.e. dynamic mesh, is done by invoking the dynamicMotionSolverFvMesh class and using the sixDoFRigidBodyMotion solver. The mesh points are then updated according to the motion of the rigid body, by solving the Laplacian of the mesh displacement. In doing so, the displacement of the cells adjacent to the rigid body is diffused to the surrounding mesh. The reader is referred to Urquhart, [10] for an example of its implementation. Using this method, Maruai *et al.,* [25] successfully simulated the transverse vibration of a square cylinder with a downstream splitter plate in a 2D flow domain.

However, diffusion of the cell displacement due to the motion of the rigid body is severely restricted when the rigid body is moving very close to a wall. An SVIV simulation falls under this category, as the vibration only sets in when $s^* < 0.25$. Koide *et al.,* [22] used two values of s^*: 0.08 and 0.16 in their experiments and attempting to simulate these conditions will cause the cell displacement to be highly concentrated within this gap. An immediate consequence of this is that the mesh becomes highly skewed [12,13] giving negative volumes and introducing severe conservation errors. A snapshot of a severely deformed mesh next to the strip-plate is given in Fig. **2**, causing the simulation to halt at 0.4 s of flow time. To circumvent this problem, Ding *et al.,* [12] and

Ding *et al.,* [13] used a generalized grid interface (GGI) [8] to allow a sliding mesh interface between two regions interfaced with non-conforming patches.

In the latest version of OpenFOAM (either OpenFOAM v5.0, or OpenFOAM-dev), GGI is implemented under the name arbitrary mesh interface (AMI) and arbitrarily coupled mesh interface (ACMI). The principle and implementation of both AMI and ACMI are discussed in the next subsection.

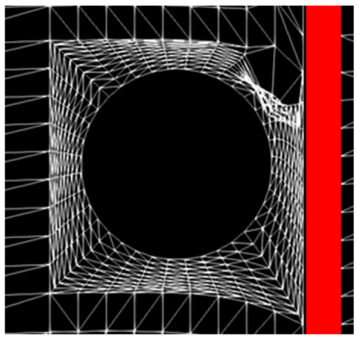

Fig. 2. Example of severe deformation of mesh within the small gap between the cylinder and strip-plate. The red rectangle is the strip-plate

2.3 Sliding Mesh Interface in Openfoam Using AMI And ACMI

OpenFOAM supported the usage of AMI and ACMI since version 2.1.0, and ACMI since version 2.3.0. The idea behind the usage of A(C)MI is that patches no longer need to be conforming, and overlapping patches contribute their transport quantities to the neighbour patch according to the fraction of overlapping area [37].

Fig. **3** shows the schematic of the ACMI implementation. The principal patches in this schematic are patches A and B. The ancillary patch is patch E. Regions C and D are where the principal patch overlaps the ancillary, each overlapping 25% of the area of patch E. As such, patches A and B only contributes 25% each of their transport quantities to patch E. This principle is true both in AMI and ACMI handling. The difference between AMI and ACMI is in the treatment of non-overlapping sub-patches. When using ACMI, the non-overlapping part of patch E, i.e. top half, can be set to another boundary type - thus integrating two types of boundary treatment within one patch.

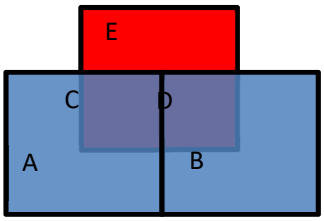

Fig. 3. Schematic of ACMI implementation. The non-overlapping sub-patch E can be designated as a wall

By implementing ACMI, the mesh on the cylinder side slides on top of the strip-plate side, preventing the severe deformation of the surrounding mesh. This is shown in Greenshields, [37]. With the successful implementation of ACMI, we can now set up our simulation case. The details of the simulation are given in the next section.

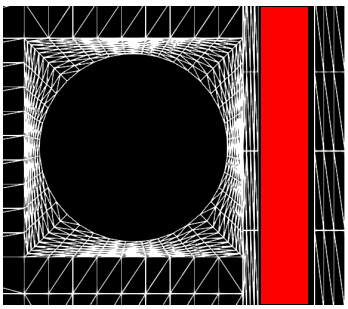

Fig. 4. Successful implementation of ACMI at the gap between the upstream cylinder and strip-plate

3. Simulation Setup

We are simulating the occurrence of SVIV as experimented by Koide *et al.,* [22]. The value of $D = 10$ mm, $s^* = 0.16$, and the downstream bluff body is a strip-plate of width $w = 10$ mm and thickness $t = 3$ mm. Other mechanical and fluid properties follow as reported by Koide *et al.,* [22].

The simulation domain extends 10 diameters (10D) from the top, bottom and upstream surfaces of the circular cylinder. The domain extends 20D from the downstream surface of the circular cylinder. In the lateral direction (direction towards normal to the x-y plane in Fig. **5**), the domain extends 10D from the sides of the circular cylinder in either direction. The total number of cells is in the order of 3×10^5 cells. The freestream velocity $U = 1.0$ m/s is chosen as the representative case where SVIV becomes detectable. This is equivalent to $U^* = 22.7$.

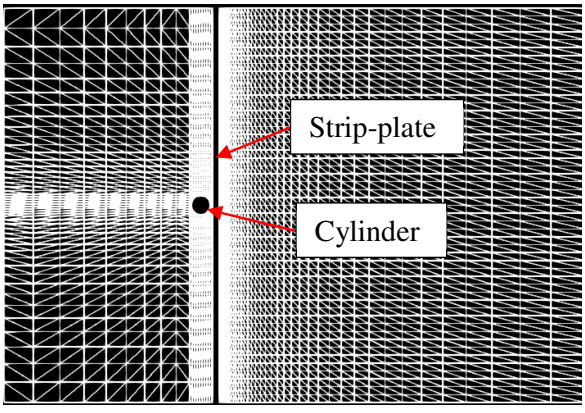

Fig. 5. The mesh used in this study. Note that the strip-plate extends from the bottom to the top of the simulation domain

As the actual flow condition under which SVIV takes place is turbulent, a Reynolds averaged Navier-Stokes (RANS) approximation of the turbulence is implemented to offset the computational cost. The one-equation model of Spalart-Allmaras [1,33,39] is chosen as it has a reasonable record of

capturing the flow dynamics, and amplitude and frequency response of a circular cylinder excited by Karman vortex, i.e. Karman vortex-induced vibration (KVIV). There is also an obvious advantage against 2 or more equation models: the Spalart-Allmaras (S-A) model only adds 1 additional equation to be solved, hence being less computationally expensive. Implementation of the S-A model in OpenFOAM is done by switching the turbulence model from laminar to RANS and determining the levels of ν_T and $\tilde{\nu}$ through algebraic equations as reported by Langley Research Centre, [39].

The dynamic mesh handling is done by the dynamicMotionSolverFvMesh class, and the solver used for the motion of the cylinder is the sixDoFRigidBodyMotion. A solution of the 3D transient flow field is done using the pimpleDyMFoam application, which handles the solution of pressure and cell displacement using generalized geometric-algebraic multi-grid (GAMG) solver, while the velocity and turbulence viscosity are solved using the stabilized preconditioned biconjugate gradient (PBiCGStab) method.

4. Results and Discussion

The reader is first and foremost reminded that the sole objective of this simulation is to test the case setup using OpenFOAM that implements ACMI and the one-equation turbulence model S-A and make sure that it will not generate errors midway. This is a crucial step before the case can be productively run on a computer cluster, as it minimizes the loss of computing time while accessing a high-performance computing (HPC) cluster due to preventable debugging efforts.

We run the simulation for 1060-time steps, with 1-time step equivalent to 0.0001 s of flow time. We present the velocity magnitude field in the $y/D = 0$ plane in Fig. **6**. The velocity immediately downstream the cylinder is seen to be near zero at the sides of the cylinder (cylinder ends), and this extends towards the middle of the cylinder with a length of approximately one-third the cylinder length ($= l/3$). However, even at this early stage of flow development (1.06 s of flow time), we can already identify a region of high velocity (≈ 1 m/s) located at approximately the middle one-third of the cylinder. This is quite possibly the initial stages of the streamwise vortex formation. Fig. **7** shows the same occurrence, but in the $y/D = 0.5$ plane in which is the plane at the top surface of the cylinder.

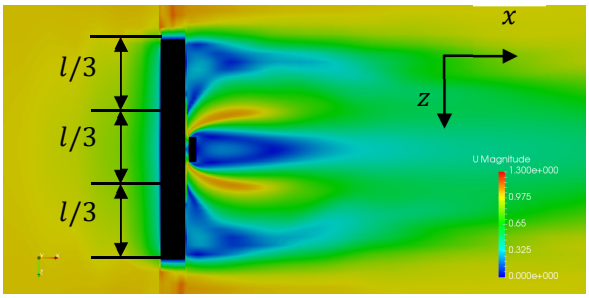

Fig. 6. The velocity magnitude field around the circular cylinder and strip-plate in the $y/D = 0$ plane. The velocities range from 0 m/s (blue) to 1.3 m/s (red)

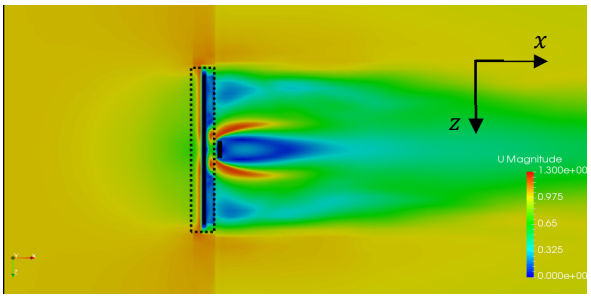

Fig. 7. The velocity magnitude field at $\boldsymbol{y/D = 0.5}$ (top of the cylinder). The dashed line gives the outline of the upstream cylinder

The most important facet of this result is, however, the fact that the application of ACMI successfully mitigated the severe distortion of the mesh around the juncture between cylinder and strip-plate and allowed the simulation to progress unimpeded.

Admittedly, the mesh in this test simulation is yet to be refined to convergence, and the flow time is yet to be lengthened to a stable solution. But as can be implied by Travin *et al.*, [38], when testing the application of a new method/simulation setup, grid convergence can be of secondary importance vis-à-vis confirming the applicability of the method/simulation setup itself. The refinement of the spatial and temporal discretization and the extension of flow time towards a stable solution can always be done promptly after.

4. Conclusions

In this study, we argued the valuableness of SVIV as the mechanism to drive energy harvesting from flows to sensor networks. We reviewed the literature to establish the parameters that affect the amplitude and frequency response of the SVIV system. We also argued for a wider adoption of CFD as a tool to study SVIV by discussing the potential setups available to the user of the open source CFD toolbox OpenFOAM, to tackle FSI problems.

As a result, we found that aspects of the flow that is critical to the behaviour of SVIV that is 2, or 3 dimensional are generally left out, presumably due to the high initial investment of capital required. We showed the potential of OpenFOAM as a practical solution to this problem by reviewing the working principle of A(C)MI, which lies at the core of a successful simulation involving a sliding mesh. Finally, we demonstrated the applicability of ACMI in simulating the near-wall FSI problem of SVIV, and the simulation results are indicative of the valuable output that can be expected with the further convergence of the solution.

Acknowledgement

The first author acknowledges the Malaysian Ministry of Higher Education and Universiti Malaysia Sarawak for the conferment of a PhD scholarship. This work is supported by the FRGS grant from MOHE numbered R.K130000.7843.4F712.

References

[1] Allmaras, Steven R., and Forrester T. Johnson. "Modifications and clarifications for the implementation of the Spalart-Allmaras turbulence model." In *Seventh international conference on computational fluid dynamics (ICCFD7)*, pp. 1-11. 2012.

[2] ANSYS. n.d. “ANSYS User Guide.” Meshing User’s Guide. Accessed July 25, 2018.

[3] Azimoh, Chukwuma Leonard, Patrik Klintenberg, Fredrik Wallin, and Björn Karlsson. "Illuminated but not electrified: An assessment of the impact of Solar Home System on rural households in South Africa." *Applied energy* 155 (2015): 354-364.
[4] Azimoh, Chukwuma Leonard, Fredrik Wallin, Patrik Klintenberg, and Björn Karlsson. "An assessment of unforeseen losses resulting from inappropriate use of solar home systems in South Africa." *Applied energy* 136 (2014): 336-346.
[5] Aziz, Nor Azlina Ab, and Kamarulzaman Ab Aziz. "Managing disaster with wireless sensor networks." In *Advanced Communication Technology (ICACT), 2011 13th International Conference on*, pp. 202-207. IEEE, 2011.
[6] Bae, Heon Meen, László Baranyi, Mizuyasu Koide, Tsutomu Takahashi, and Masataka Shirakashi. "Suppression of Kármán vortex excitation of a circular cylinder by a second cylinder set downstream in cruciform arrangement." *Journal of Computational and Applied Mechanics* 2, no. 2 (2001): 175-188.
[7] Bae, Heon Meen, Takao Hirai, Masatoshi Sano, and Masataka Shirakashi. 1992. "Excitation by Vortices Shedding Periodically from Two Cylinders in Cruciform Arrangement." Transactions of the Japan Society of Mechanical Engineers Series B 58 (551).
[8] Beaudoin, Martin, and Hrvoje Jasak. "Development of a generalized grid interface for turbomachinery simulations with OpenFOAM." In *Open source CFD International conference*, vol. 2. Berlin, 2008.
[9] Beeby, S. P, M. J Tudor, and N. M. White. "Energy harvesting vibration sources for microsystems applications." *Measurement science and technology* 17, no. 12 (2006): R175.
[10] Urquhart, Magnus. 2015. "Proceedings of CFD with OpenSource Software." In A Tutorial of the SixDofRigidBodyMotion Library with Multiple Bodies, edited by Håkan Nilsson. Gothenburg.
[11] Jabatan Perdana Menteri. 2014. "Economic Transformation Programme Annual Report 2014." http://www.teraju.gov.my/laporan-tahunan-etp-2014/?lang=en.
[12] Ding, Lin, Michael M. Bernitsas, and Eun Soo Kim. "2-D URANS vs. experiments of flow induced motions of two circular cylinders in tandem with passive turbulence control for 30,000< Re< 105,000." *Ocean Engineering* 72 (2013): 429-440.
[13] Ding, Lin, Li Zhang, Eun Soo Kim, and Michael M. Bernitsas. "URANS vs. experiments of flow induced motions of multiple circular cylinders with passive turbulence control." *Journal of Fluids and Structures* 54 (2015): 612-628.
[14] Discenzo, Fred M., Dukki Chung, and Kenneth A. Loparo. "Power scavenging enables maintenance-free wireless sensor nodes." In *Proceedings of the 6th international conference on complex systems*. 2006.
[15] Fox, T. A. "Interference in the wake of two square-section cylinders arranged perpendicular to each other." *Journal of Wind Engineering and Industrial Aerodynamics* 40, no. 1 (1992): 75-92.
[16] Huang, Rong Fung, Ching Min Hsu, and Wei Cheng Lin. "Flow characteristics around juncture of a circular cylinder mounted normal to a flat plate." *Experimental Thermal and Fluid Science* 55 (2014): 187-199.
[17] Kawabata, Yusuke, Tsutomu Takahashi, Takeshi Haginoya, and Masataka Shirakashi. "Interference effect of downstream strip-plate on the crossflow vibration of a square cylinder." *Journal of Fluid Science and Technology* 8, no. 3 (2013): 348-363.
[18] Koide, M., N. Kato, Tsutomu Takahashi, and Masataka Shirakashi. "Vibration Control for a Circular Cylinder by a Strip-Plate Set Downstream in Cruciform Arrangement: 2nd Report, Generation and Suppression of Vortex Excitation on Elastically Supported Cylinder." *Transactions of The Japan Society of Mechanical Engineers Series B* 75, no. 752 (2009): 691-699.
[19] Koide, Mizuyasu. "Influence of a cruciform arrangement downstream strip-plate on crossflow vibration of a square cylinder." *Journal of Computational and Applied mechanics* 8, no. 2 (2007): 135-148.
[20] Koide, Mizuyasu, Katsuji Oogane, Tsutomu Takahashi, and Masataka Shirakashi. 2004. "Experimental Study on Universality of Longitudinal Vortices Shedding Periodically from Crisscross Circular Cylinder System in Uniform Flow." Transactions of the Visualization Society of Japan 24 (4): 15–22.
[21] Koide, Mizuyasu, Takahiro Sekizaki, Syuichi Yamada, Tsutomu Takahashi, and Masataka Shirakashi. "A Novel Technique for Hydroelectricity Utilizing Vortex Induced Vibration." In *ASME 2009 Pressure Vessels and Piping Conference*, pp. 279-288. American Society of Mechanical Engineers, 2009.
[22] Koide, Mizuyasu, Takahiro Sekizaki, Shuichi Yamada, Tsutomu Takahashi, and Masataka Shirakashi. "Prospect of micro power generation utilizing VIV in small stream based on verification experiments of power generation in water tunnel." *Journal of Fluid Science and Technology* 8, no. 3 (2013): 294-308.
[23] Mackowski, A. W., and C. H. K. Williamson. "An experimental investigation of vortex-induced vibration with nonlinear restoring forces." *Physics of Fluids* 25, no. 8 (2013): 087101.
[24] Maric, Tomislav, Jens Hopken, and Kyle Mooney. "The OpenFOAM technology primer." (2014).
[25] Maruai, Nurshafinaz Mohd, Mohamed Sukri Mat Ali, Mohamad Hafiz Ismail, and Sheikh Ahmad Zaki Shaikh Salim. "Downstream flat plate as the flow-induced vibration enhancer for energy harvesting." *Journal of Vibration and Control* (2017): 1077546317707877.

[26] Nguyen, Tuananh, Mizuyasu Koide, Tsutomu Takahashi, and Masataka Shirakashi. "Universality of longitudinal vortices shedding from a cruciform two circular cylinder system in uniform flow." *Journal of Fluid Science and Technology* 5, no. 3 (2010): 603-616.
[27] Nguyen, T., M. Koide, S. Yamada, T. Takahashi, and M. Shirakashi. "Influence of mass and damping ratios on VIVs of a cylinder with a downstream counterpart in cruciform arrangement." *Journal of Fluids and Structures* 28 (2012): 40-55.
[28] Open, F. O. A. M. "The open source CFD Toolbox User guide." (2014).
[29] Jabatan Perdana Menteri. 2014. "Economic Transformation Programme Annual Report 2014."
[30] Remacle, J. F., C. Geuzaine, G. Compère, and E. Marchandise. 2010. "High Quality Surface Remeshing Using Harmonic Maps." International Journal for Numerical Methods in Engineering 83 (4): 403–25.
[31] Remacle, J-F., Jonathan Lambrechts, Bruno Seny, Emilie Marchandise, Amaury Johnen, and C. Geuzainet. "Blossom-Quad: A non-uniform quadrilateral mesh generator using a minimum-cost perfect-matching algorithm." *International journal for numerical methods in engineering* 89, no. 9 (2012): 1102-1119.
[32] Shirakashi, M., K. Mizuguchi, and H. M. Bae. "Flow-induced excitation of an elastically-supported cylinder caused by another located downstream in cruciform arrangement." *Journal of Fluids and Structures* 3, no. 6 (1989): 595-607.
[33] Spalart, PRaA, and S1 Allmaras. "A one-equation turbulence model for aerodynamic flows." In *30th aerospace sciences meeting and exhibit*, p. 439. 1992.
[34] Sun, Hai, Eun Soo Kim, Gary Nowakowski, Erik Mauer, and Michael M. Bernitsas. "Effect of mass-ratio, damping, and stiffness on optimal hydrokinetic energy conversion of a single, rough cylinder in flow induced motions." *Renewable Energy* 99 (2016): 936-959.
[35] Sun, Hai, Chunhui Ma, Eun Soo Kim, Gary Nowakowski, Erik Mauer, and Michael M. Bernitsas. "Hydrokinetic energy conversion by two rough tandem-cylinders in flow induced motions: Effect of spacing and stiffness." *Renewable energy* 107 (2017): 61-80.
[36] Takahashi, Tsutomu, Laszlo Baranyi, and Masataka Shirakashi. "Configuration and frequency of longitudinal vortices shedding from two circular cylinders in cruciform arrangement." *Journal of the Visualization Society of Japan* 19, no. 75 (1999): 328-336.
[37] Greenshields, Chris. 2014. "OpenFOAM 2.3.0: Arbitrary Mesh Interface." 2014.
[38] Travin, Andrei, Michael Shur, Michael Strelets, and Philippe Spalart. "Detached-eddy simulations past a circular cylinder." *Flow, Turbulence and Combustion* 63, no. 1-4 (2000): 293-313.
[39] Langley Research Centre. 2018. "Turbulence Modeling Resource." Turbulence Modeling Resource. 2018.
[40] Van Oudheusden, B. W., F. Scarano, N. P. Van Hinsberg, and E. W. M. Roosenboom. "Quantitative visualization of the flow around a square-section cylinder at incidence." *Journal of Wind Engineering and Industrial Aerodynamics* 96, no. 6-7 (2008): 913-922.
[41] Westerweel, Jerry. "Fundamentals of digital particle image velocimetry." *Measurement science and technology* 8, no. 12 (1997): 1379.
[42] Xia, Feng, Laurence T. Yang, Lizhe Wang, and Alexey Vinel. "Internet of things." *International Journal of Communication Systems* 25, no. 9 (2012): 1101-1102.
[43] Yen, Shun C., and Chen W. Yang. "Flow patterns and vortex shedding behavior behind a square cylinder." *Journal of Wind Engineering and Industrial Aerodynamics* 99, no. 8 (2011): 868-878.
[44] Kausar, ASM Zahid, Ahmed Wasif Reza, Mashad Uddin Saleh, and Harikrishnan Ramiah. "Energizing wireless sensor networks by energy harvesting systems: Scopes, challenges and approaches." *Renewable and Sustainable Energy Reviews* 38 (2014): 973-989.
[45] Zdravkovich, M. M. "Interference between two circular cylinders forming a cross." *Journal of Fluid Mechanics* 128 (1983): 231-246.